Influence of Radiation on Product Yields in a Film Boiling Reactor

C. Thomas Avedisian, Wing Tsang, Terence Davidovits, and Jonah R. Allaben

Sibley School of Mechanical and Aerospace Engineering, Cornell University, Ithaca, New York, NY 14853

Introduction

The film boiling reactor (FIBOR)[1] is analyzed to show the influence of radiation across the vapor film on product yields. The geometry is that of a horizontal, catalyst-coated, tube suspended in a pool of saturated methanol at atmospheric pressure. The vapor film surrounding the heated tube is the reacting volume and surface reactions are treated with an Arrhenius form of the reaction rate. Previous analysis on film boiling without catalytic reaction on a horizontal tube showed the influence of surface emission.[2–5] When coupled with catalytic decomposition, film boiling analysis has neglected radiative effects.[1,6] In this note we set limits to this assumption.

We begin by outlining the model for film boiling with chemical reaction and present results for a horizontal tube with wall temperatures ranging from the minimum film boiling temperature needed to support a vapor film (450 K for methanol) to 1800 K though most catalysts will decompose well before this upper limit and practical operational limits may be under 1000 K. The present calculations are designed to show general trends at high temperatures where radiation may be important. The species diffusion process is derived from the previously presented analysis.[1] All of the assumptions of that analysis are adopted here with the addition of those specific to radiation as discussed in the Analysis section. We first consider the case where radiation is entirely determined by surface emission between the tube wall and liquid/vapor interface and neglect volumetric absorption and emission; we then consider the effects of volumetric absorption and emission in the vapor film.

Analysis

Surface emission with negligible gaseous absorption and emission

Radiation across the vapor film influences heat transfer through an energy balance on a control volume in the vapor film which neglects kinetic energy as

$$\int_A \rho h \overline{v} \bullet \overline{n} dA = \int_A \overline{q}'' \bullet \overline{n} dA \tag{1}$$

where the heat flux is the sum of contributions from conduction and radiation, which can be expressed as

$$\overline{q}'' \bullet \overline{n} = \frac{k_v \Delta T_{sat}}{\delta}(1 + G) \tag{2}$$

G is a measure of the importance of surface emission from the tube wall with

$$G = C_r \delta \tag{3a}$$

where

$$C_r = \frac{\varepsilon \sigma (T_w^4 - T_{sat}^4)}{k_v \Delta T_{sat}} \tag{3b}$$

For $G \ll 1$ surface emission is negligible compared to conduction across the vapor film and the analysis reduces to that of Urban et al.[1] With Eqs. 2 and 3, Eq. 1 can be expressed as

$$\rho_v \int_0^\delta u\{L + c_{pv}(T - T_{sat})\}dz = \frac{d}{2}\int_0^\phi \left(\frac{k_v \Delta T_{sat}}{\delta}(1 + G)\right)d\phi \tag{4}$$

The mass weighted average velocity in the ϕ direction (u) and temperature distribution across the vapor film (T) are based on the condition that $Pr\ Re_\delta (\delta/\chi)^2 \ll 1$. This limit leads to simplified momentum and energy equations, with corresponding velocity and temperature profiles across the vapor film given by

$$u = \frac{g(\rho_1 - \rho_v)}{2\mu_v}\ \sin\phi(\delta z - z^2) \qquad (5)$$

and a linear temperature distribution across the vapor film,

$$T = T_{\mathrm{w}} - \Delta T_{\mathrm{sat}}\frac{z}{\delta} \qquad (6)$$

where z is the distance measured from the tube surface, $\Delta T_{\mathrm{sat}} = T_{\mathrm{w}} - T_{\mathrm{sat}}$ and a no-slip boundary condition is assumed at the liquid/vapor interface (the analysis neglects liquid motion and $v = 0$ at $y = \delta$ as discussed in Ref. 1).

Substituting Eqs. 5 and 6 into 4 gives

$$\frac{\delta^3\ \sin\phi}{3B} = \int_0^\phi \left(\frac{1}{\delta}\right)(1 + G)d\phi \qquad (7)$$

which is an integral equation. Differentiating Eq. 7 with respect to ϕ yields

$$\frac{dx}{d\phi} + \frac{4}{3}x\ \cot\phi = 4Bcsc\phi \cdot (1 + C_{\mathrm{r}}x^{1/4}) \qquad (8)$$

where $x = \delta^4$, $G = C_{\mathrm{r}}\,x^{1/4}$, and B is given by

$$B = \frac{4c_{\mathrm{pv}} \cdot \Delta T_{\mathrm{sat}}}{2L + c_{\mathrm{pv}} \cdot \Delta T_{\mathrm{sat}}} \cdot \frac{\frac{k_{\mathrm{v}}}{c_{\mathrm{pv}}\rho_{\mathrm{v}}} \cdot \frac{\mu_{\mathrm{v}}}{\rho_{\mathrm{v}}}}{g\left(\frac{\rho_1 - \rho_{\mathrm{v}}}{\rho_{\mathrm{v}}}\right)}d \qquad (9)$$

when $G \ll 1$ (no surface emission) Eq. 8, with the condition that $\left.\frac{d\delta}{d\phi}\right|_{\phi=0} = 0$ or equivalently (from Eq. 8) that, $\lim_{\phi \to 0}\left(\frac{dx}{d\phi}\right) = 0$, has an analytical solution[1,6]:

$$\delta = \sqrt{2}B^{1/4}\frac{\left(\int_0^\phi \sin^{1/3}(\phi)d\phi\right)^{1/4}}{\sin^{1/3}(\phi)} \qquad (10)$$

Otherwise, the solution to Eq. 8 must be obtained numerically using the condition for x at $\phi = 0°$ (where $x = x_{\mathrm{o}}$ and $\lim_{\phi \to 0}\left(\frac{dx}{d\phi}\right) = 0$, from Eq. 8) that

$$x_{\mathrm{o}} - 3B(1 + C_{\mathrm{r}}x_{\mathrm{o}}^{1/4}) = 0 \qquad (11)$$

A fourth order Runge-Kutta numerical method was used to solve Eq. 8 with x_{o} given by Eq. 11. To test the accuracy of the numerical solution, Eq. 10 was compared with the numerical solution of Eq. 8. The results agreed to less than 1% deviation over the ranges 450 K < T_{w} < 1800 K and 0 < ϕ < 179°.

The particular reaction considered is catalytic decomposition of methanol with the overall reaction $CH_3OH \to CO + 2H_2$ (i.e., two moles of hydrogen form at the expense of one mole of methanol). The rate constants for this reaction were taken from Ref. 6 based on measured heat transfer coefficients of a catalyst-coated tube in film boiling in methanol and plug flow reactor data. It is important to note that in this model we do not consider degradation of the catalyst (e.g., Pt-black) during operation of the FIBOR which, nonetheless, can be an important consideration in practice. The hydrogen yield is related to the mass fraction of methanol at the tube surface as

$$M_{0-\phi,H_2}^* = \varpi_{H_2}\frac{d}{2}\int_0^\phi Y_{CH_3OH,w}d\phi \qquad (12a)$$

where[1]

$$\varpi_{H_2} \sim \left(C\ e^{-\frac{E}{R_{\mathrm{o}}T_{\mathrm{w}}}}\right) \qquad (12b)$$

E is the activation energy of the reaction, C is the frequency factor of the reaction, and $Y_{CH_3OH,w}$ is the mass fraction of methanol at the tube surface ($z = 0$) which depends on ϕ.

The procedure for determining $Y_{CH_3OH,w}$ in Eq. 12a when radiation is included is operationally identical to when radiation is neglected.[1] The analysis differs from Ref. 1 by the presence of $G = C_{\mathrm{r}}\delta \neq 0$ in Eq. 8 and consideration of volumetric absorption in the vapor film. An integral method is used to analyze transport of species in the vapor film with third order polynomials assumed for the chemical species across the film. This approximation is the simplest approach consistent with satisfying boundary conditions at both the tube wall and liquid/vapor interface to give a reasonable functional form for the species distribution across the vapor film. The third order polynomial assumption satisfies four boundary conditions, two each at the solid/vapor and vapor/liquid interfaces. Integral methods in which distributions (e.g., of concentration) are assumed as in the case here may suppress errors in the computed yields (Eq. 12a). Furthermore, the predictions are strongly dependent on the reaction rate appropriate for the catalyst under consideration (e.g., Eq. 12b). Rate constants and parameters are formally independent properties of the system. However, the actual physical and chemical effects are a manifestation of the complex interaction between transport, radiation and chemistry. In that sense, the rate constants and parameters are tied to the model. More detailed analyses for species diffusion may not be any more accurate than the rate constants used to predict product yields.

Absorbing and emitting gas

The inclusion of volumetric absorption and emission in the vapor film complicates the analysis because the temperature distribution across the vapor film is then no longer given by the linear form of Eq. 6. A comparatively simple approach is taken which assumes the gas to be optically thin such that $\tau \ll 1$ where $\tau = \delta\kappa$ and κ is the Planck mean absorption coefficient (m^{-1}) which depends on temperature and gas composition. κ can be calculated from the gas temperature T, and the mole fractions of CO and CH_3OH as a molar average of the individual species absorption coefficients κ_i,[7]
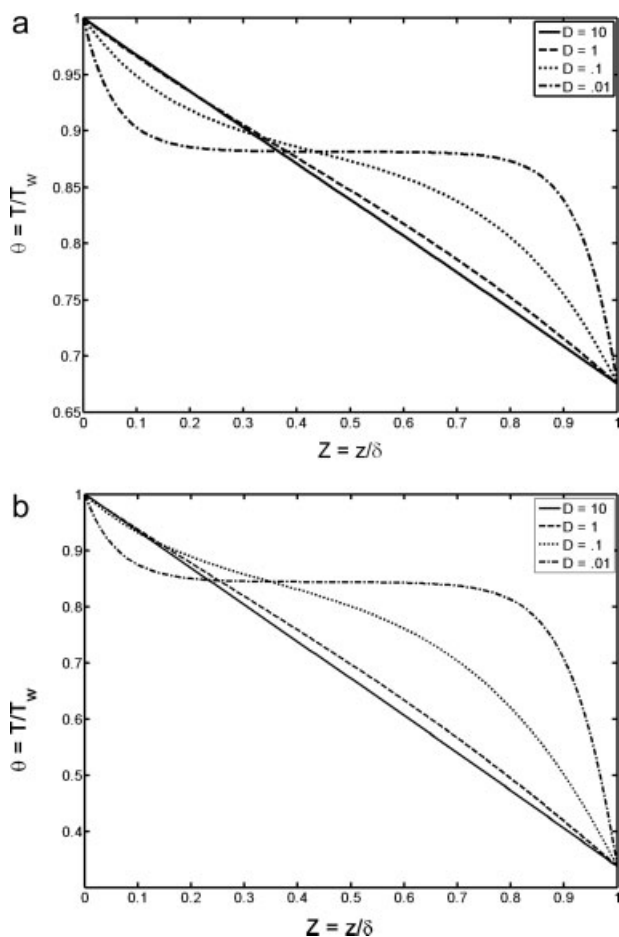
Figure 1. (a) Variation of gas temperature across the vapor film for T_w = 500 K.

Deviations from the conduction limit (linear variation) are observed for $D < 1$. (b) Variation of gas temperature across the vapor film for T_w = 1000 K. Deviations from the conduction limit (linear variation) are observed for $D < 1$.

$$\kappa_i = \frac{\int_0^\infty \kappa_{i\lambda} e_{b\lambda} d\lambda}{\sigma T^4} \tag{13}$$

The data for $\kappa_{i\lambda}(T)$[8] show that for CO and CH_3OH a conservative (e.g., high) estimate for the gas mixture absorption coefficient ranges from 17 m^{-1} to about 26 m^{-1} at room temperature. Given that our results show that δ is under about 2 mm (except for the singularity at $\phi = 180°$) the optically thin assumption is reasonable for almost the entire circumference of the tube surface.

The temperature distribution across the vapor film in the optically thin limit[7] can be put in the following non-dimensional form

$$D\frac{d^2\theta}{dZ^2} = \theta^4 - \frac{1}{2}\theta_s^4 - \frac{1}{2} \tag{14}$$

where we define D as

$$D = \frac{k}{4\sigma T_w^3 \kappa \delta^2} \tag{15}$$

and $Z = \frac{z}{\delta}$, $\theta = \frac{T}{T_w}$, and $\theta_s = \frac{T_{sat}}{T_w}$. D is a measure of the relative importance of volumetric absorption and emission to conduction: for large D gaseous absorption and emission are negligible, conduction across the film thickness dominates heat transfer, and a linear temperature distribution results (e.g., Eq. 6); as D decreases, the temperature distribution becomes progressively nonlinear indicating that the gas absorbs and emits.

Results

Two parameters govern the importance of radiation: one for surface emission (G) and the other for volumetric absorption (D). We first consider volumetric absorption.

Equation 14 is a nonlinear differential equation with no closed form solution. However, Eq. 14 can be solved numerically by itself if D is considered a parameter. Doing so allows determining the conditions under which volumetric absorption are important. That is, if the solution of Eq. 14 results in a linear temperature profile, conduction dominates and the analysis can neglect volumetric absorption; otherwise, it must be considered. We first present the solution to Eq. 14 for a range of D then determine which are most relevant to a FIBOR, using the example of methanol decomposition considered here.

Figure 1 shows the numerical solution of Eq. 14 for $0 < Z < 1$ (i.e., $0 < z < \delta$) using a collocation method. For $D = 10$, the temperature distribution is linear which signifies that volumetric absorption is negligible. Slight deviations are observed for $D = 1$ and significant difference from a linear profile are seen for $D \leq 0.1$ for both $T_w = 500$ K (Figure 1a) and 1000 K (Figure 1b). Figure 2 shows the variation of D with parameters based on Eq. 15. We simply varied δ over the range in the figure to obtain the result shown. The numerical solution shows δ to be within the range depicted in the figure. For all combinations of conditions above the horizontal line ($D = 1$) absorption is negligible.
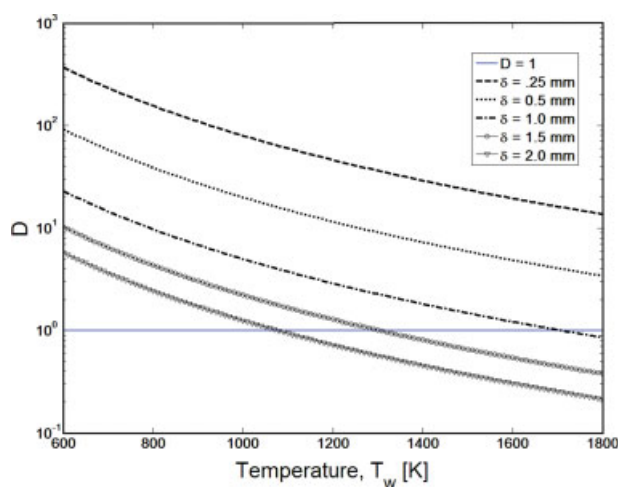
Figure 2. Variation of D with T_w at the indicated δ.

For conditions above the blue line ($D = 1$), volumetric absorption in the vapor film is negligible (cf, Figure 1). [Color figure can be viewed in the online issue, which is available at www.interscience.wiley.com.]
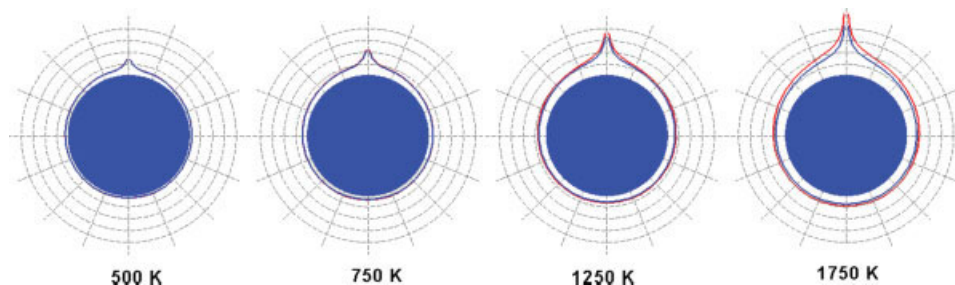
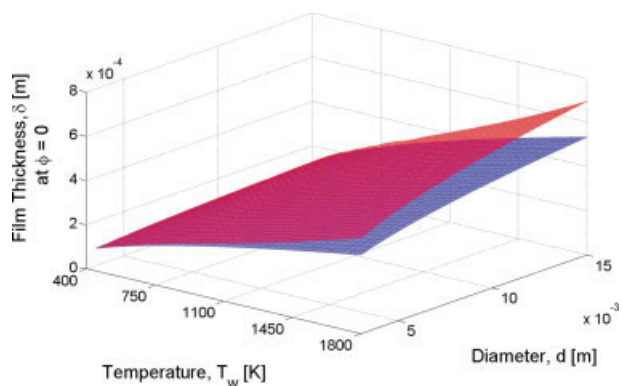**Figure 3. Scale depiction of vapor film thickness around a 5 mm diameter tube at the indicated value of T_w.**

Divisions are in 0.5 mm and 22.5° increments. Red line includes radiation; blue line neglects radiation. For 500 and 750 K cases, results are virtually coincident. [Color figure can be viewed in the online issue, which is available at www.interscience.wiley.com.]

Considering the practical operational limits of a FIBOR, a lower bound of D using Eq. 14 is obtained from the lowest value of k and highest (reasonable) values of T_w, κ and δ for a gas film comprised of methanol, CO and H_2. We estimate that $k \sim 0.03$ W/mK (methanol[9]), $\kappa \sim 26m^{-1}$ using Eq. 13 and data from,[8] $\delta < 2$ mm, and $T_w < 1800$ K as an upper value limited by the melting temperature of the tube material (e.g., stainless steel). With these estimates we find that $D > 5.7$ which is the smallest value that is relevant to present conditions. Figure 1 shows that even for $D = 1$ which is already too low based on the above estimate, the temperature distribution is nearly linear. As a result, for the parameter values considered here there are no conditions where volumetric absorption would be important when using methanol as the reactant liquid. Under this circumstance, the solution of Eq. 14 is in effect given by Eq. 6 (as $\phi = 180° Y_{CH_3OH,w}$ decreases so that from Eq. 12a the contribution from the region around $\phi = 180°$ may also be small). Also, when volumetric absorption is negligible, the chemical reaction process itself has no influence on radiation because the absorption coefficient which is influenced by the product species does not then enter into the analysis.

Considering only surface emission from the tube with $\varepsilon = 1$ in Eq. 3b for illustration (e.g., formulations in the Sur-

face Emission with Negligible Gaseous Absorption and Emission section), Figure 3 shows scaled images of the structure of the vapor film around a 5 mm diameter tube at four surface temperatures. The red curve includes surface emission and the blue curve neglects radiation). At low T_w, the vapor film thickness is very close to the tube surface except for the singularity at $\phi = 180°$. Increasing T_w also increases the vapor film thickness as a higher tube temperature enhances heat transfer which in turn increases the evaporation rate and thickens δ. At high temperatures, greater than about 1000 K, the effect of radiation on the film thickness becomes noticeable, again increasing the film thickness compared to neglecting surface emission because of the added contribution to heat transfer by radiation in addition to conduction.

Figure 4 shows the variation of vapor film thickness with T_w and tube diameter at a reference position of $\phi = 0°(\delta_o)$ for both the nonradiative and the radiative cases (i.e., from Eq. 11). When surface emission is included, δ_o is larger than when radiation is neglected for the range of tube diameters shown in Figure 4, as well as for T_w above about 1000 K. At lower temperatures, radiation has almost no effect on δ


Figure 4. Variation of vapor film thickness at $\phi = 0°$ as a function of T_w and d showing the influence of radiation (red) vs. the surface emission neglected case in blue.

[Color figure can be viewed in the online issue, which is available at www.interscience.wiley.com.]
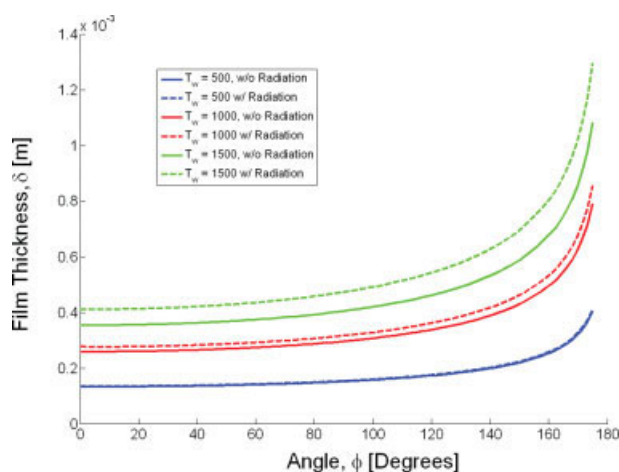
Figure 5. Influence of surface emission on vapor film thickness for three T_w for a 5 mm diameter tube: dotted lines include surface emission; solid lines neglect radiation.

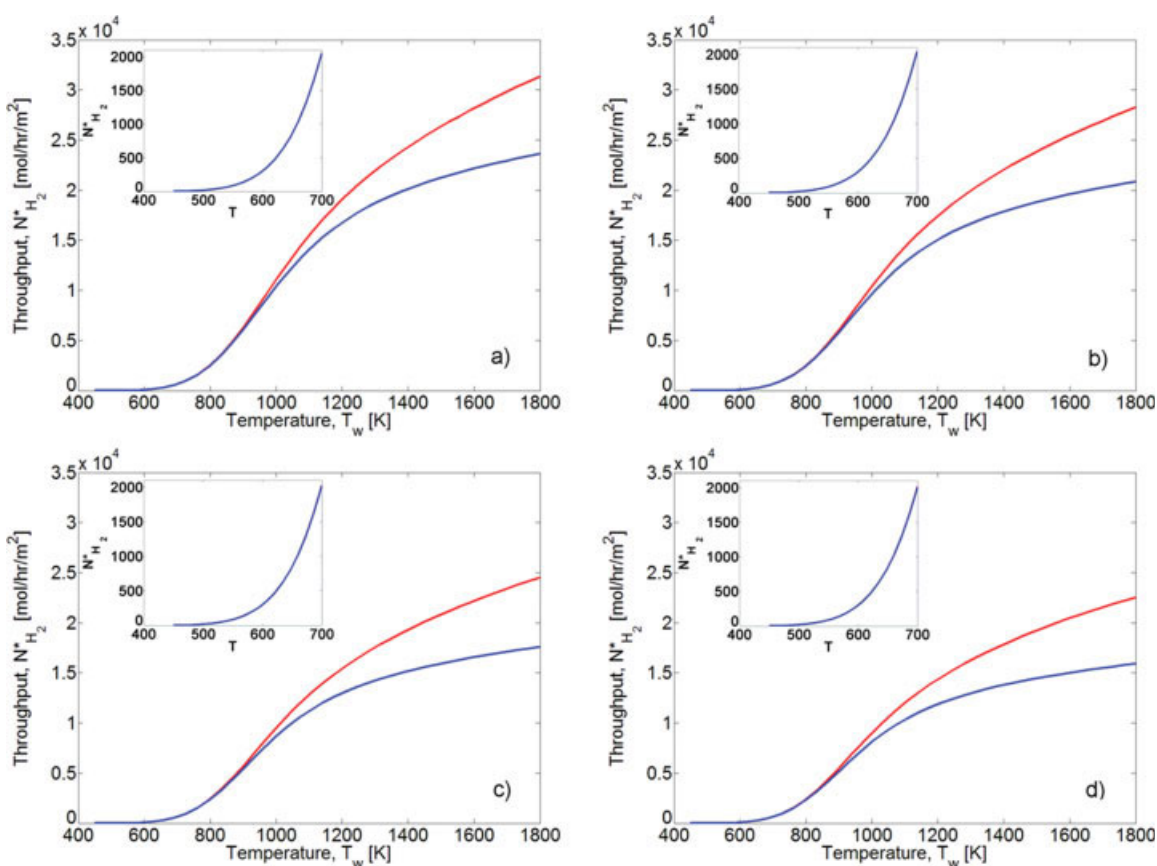[Color figure can be viewed in the online issue, which is available at www.interscience.wiley.com.]
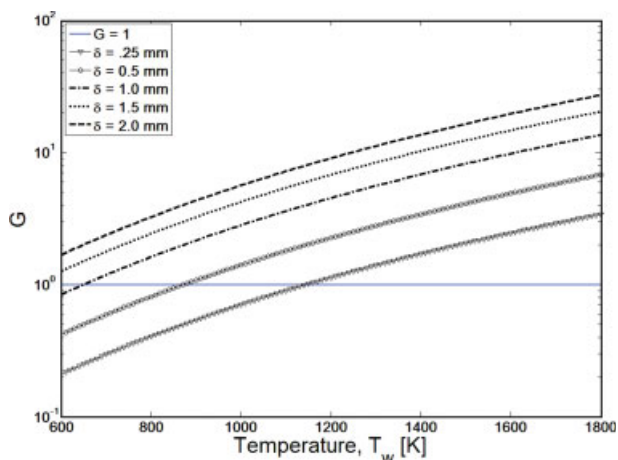
Figure 6. Variation of G with T_w at the indicated δ. For conditions below the blue line ($G = 1$), radiative emission from tube surface may be neglected.

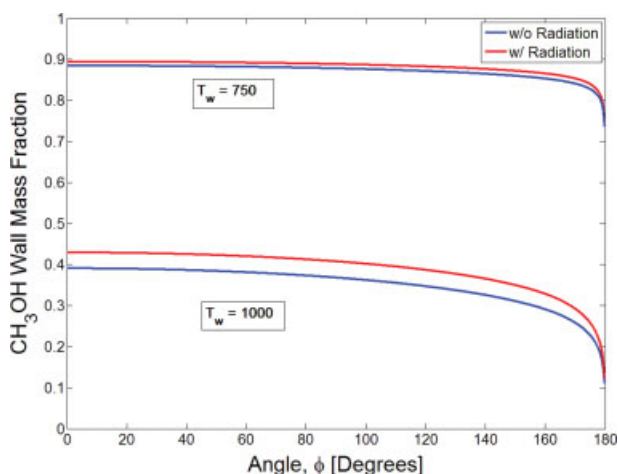[Color figure can be viewed in the online issue, which is available at www.interscience.wiley.com.]

regardless of tube diameter. Figure 5 shows the variation of δ with ϕ for T_w = 500, 1000, and 1500 K using a tube diameter of 5 mm as a reference. With increasing ϕ, δ also increases (see also Figure 3). At 500 K, the difference between the nonradiative film thickness and radiative thickness is negligible; at 1500 K, the film thickness is 15% larger when surface emission is included. These effects are again attributed to increased heat transfer to the liquid/vapor interface by including radiation compared to neglecting radiation, and to the resulting effect of this increase on evaporation at the liquid/vapor interface.

The parameter G (Eq. 3) determines the influence of surface emission across the vapor film. Figure 6 shows how G depends on T_w. As with Figure 2, we varied δ over the range shown in Figure 6 to illustrate its influence on G. The horizontal line corresponds to conditions where surface emission and conduction exert a similar effect. For $G \gg 1$, surface emission is important; for $G \ll 1$ it is negligible. Precisely how large or small is required is determined by the specifics of the solution. For example, comparing Figures 5 and 6 it is seen that at $\phi \approx 140°$ and 1500 K, $\delta \approx 600$ μm and Figure 5 shows that there is a significant effect of radiation. From Figure 6 at these same conditions, $G \approx 4$.

Figure 7. Hydrogen yield (per unit area of tube surface) as a function of T, (a) d = 3 mm, (b) d = 5 mm, (c) d =10 mm, and (d) d = 15 mm.

Red lines include radiation and blue lines neglect radiation. Insets show predicted yields below T_w = 700 K. [Color figure can be viewed in the online issue, which is available at www.interscience.wiley.com.]

Figure 8. Variation of methanol mass fraction at tube surface for a tube diameter of 5 mm.

Red curves include radiation and blue curves neglect radiation. [Color figure can be viewed in the online issue, which is available at www.interscience.wiley.com.]

Figure 7 shows the predicted hydrogen throughput as a function of T_w and tube diameter. The hydrogen yield was computed from Eq. 12 as outlined in the surface emission with negligible gaseous absorption and emission section. Including radiation in the analysis increases $M^*_{0-\phi,H_2}$ (Eq. 12) for T_w above 1000 K but that there is virtually no effect at $T_w < 700$ K as indicated in the inset figures. Figure 8 shows the variation of $Y_{CH_3OH,W}$ with ϕ at two temperatures (750 and 1000 K) for a 5 mm diameter tube for illustration. The area under the curves shown in Figure 8 is the integral in Eq. 12a. A slight increase is evident when radiation is included (red line) compared to when radiation is neglected (blue line). This effect is due to increased evaporation of methanol when radiation is included. The higher methanol wall mass fraction at $T_w = 750$ K compared to $T_w = 1000$ K is the result of T_w strongly influencing reaction rate (Eq. 12b) such that at low temperature more methanol accumulates at the surface without being converted compared to high temperature. While $M^*_{0-\phi,H_2}$ is proportional to the area under curves like those shown in Figure 8, the higher area at lower T_w is compensated by the much stronger increase of ϖ_{H_2}(Eq. 12b) as T_w increases to produce the increase of $M^*_{0-\phi,H_2}$ with T_w shown in Figure 7.

The effect of radiation on predicted hydrogen production is, as expected, important only at relatively high temperatures here being greater than about 1000 K for the conditions of the calculations as shown in Figure 7. In practice, the operation of a FIBOR would be at temperatures which are high enough to drive product yields to appreciable levels and to maintain film boiling yet without compromising the integrity of the tube material and catalytic coating.

Concluding Remarks

The operational range of parameters is identified where radiation effects—either from surface emission from the tube wall or volumetric gaseous absorption and emission in the vapor film—should be included in the analysis of film boiling with chemical reaction. For the conditions examined here, volumetric emission is not an important consideration and surface emission from the tube influences product yields at wall temperatures only above about 1000 K. Above this temperature, including surface emission in the analysis results in higher methanol mass fractions at the tube surface, larger vapor film thicknesses, and higher product yields compared to neglecting radiation. Two nondimensional parameters are shown to determine the importance of radiation, one concerning volumetric absorption and the other concerning surface emission.

Acknowledgments

Notation

A = area (m^2)
c_{pv} = specific Heat [J/(kg K)]
d = tube diameter (m)
$e_{b\lambda}$ = spectral blackbody emissive power (W/(m^2-μm)
g = acceleration due to gravity, (m/s^2)
h = enthalpy (J/kg)
k_v = mean vapor thermal conductivity [W/(m K)]
L = latent heat (J/kg)
M^* = mass throughput of component [kg/(h m)]
$\bar{n}$ = normal vector
Pr = Prandtl number
$\vec{q}''$ = heat flux (W/m^2)
T = temperature (K)
T_w = temperature at the tube wall (K)
T_{sat} = temperature at the vapor/liquid interface, $\Delta T_{sat} = T_w - T_{sat}$ (K)
$\bar{v}$ = velocity vector [m/s]
v = vapor velocity in "y" direction
z = distance measured normal to tube surface (m)

Greek letters

δ = vapor film thickness (m)
ρ = density (kg/m^3)
ε = emissivity, dimensionless
λ = wavelength (m)
μ = viscosity [kg/(m s)]
σ = Stefan-Boltzmann constant [W/(m^2 K^4)]
ϕ = angle measured from bottom of tube (rad)
χ = arc length around tube circumference (d/2 ϕ)

Subscripts

v = vapor
l = liquid

Literature Cited

1. Urban BJ, Avedisian CT, Tsang W. Film boiling with chemical reaction: analysis of an alternative method for hydrogen production. *AIChE J*. 2006;52:2582–2595.
2. Sakurai A, Shiotsu M, Hata K. A general correlation for pool film boiling heat transfer from a horizontal cylinder to subcooled liquid. I. A theoretical pool film boiling heat transfer model including radiation contributions and its analytical solution. *J Heat Tran*. 1990;112:430–440.

3. Liu MH, Yang YM, Maa JR. A general correlation for pool film boiling heat transfer from a horizontal cylinder to saturated binary liquid mixtures. *Int J Heat Mass Tran*. 1998;41:2321–2334.
4. Nishikawa K, Ito T. Two-phase boundary-layer treatment of free-convection film boiling. *Int J Heat Mass Tran*. 1966;9:103–115.
5. Sarma PK, Subrahmanyam T, Rao VD, Bergles AE. Turbulent film boiling on a horizontal cylinder. *Int J Heat Mass Tran*. 2001;44:207–214.
6. Okuyama K, Iida Y. Film-boiling heat transfer with a catalytic decomposition reaction. *JSME Int J Ser B*. 1994;37:123–131.

7. Sparrow EM, Cess RD. *Radiation Heat Transfer, Revised Edition*. Belmont, CA: Brooks/Cole Publishing Co. 1970:20, 215, 250.
8. Butler RAH, Engler DL, Armstrong JC. The virtual planetary laboratory molecular spectroscopy database. 2007. Available at: http://vpl.ipac.caltech.edu/spectra/.
9. Vargaftik NB. *Handbook of Physical Properties of Liquids and Gases*. New York: Hemisphere Publishing, 1975:404–406,